ENPP1 Mutation Causes Recessive Cole Disease by Altering Melanogenesis

Marwa Chourabi[1,2], Mei Shan Liew[3], Shawn Lim[3], Dorra H'mida-Ben Brahim[2], Lobna Boussofara[4], Liang Dai[3], Pui Mun Wong[1], Jia Nee Foo[5], Badreddine Sriha[6], Kim Samirah Robinson[7], Simon Denil[7], John EA Common[8], Ons Mamaï[9], Youcef Ben Khalifa[10], Mathieu Bollen[11], Jianjun Liu[5], Mohamed Denguezli[4], Carine Bonnard[1], Ali Saad[2] and Bruno Reversade[1]

Cole disease is a genodermatosis of pigmentation following a strict dominant mode of inheritance. In this study, we investigated eight patients affected with an overlapping genodermatosis after recessive inheritance. The patients presented with hypo- and hyperpigmented macules over the body, resembling dyschromatosis universalis hereditaria in addition to punctuate palmoplantar keratosis. By homozygosity mapping and whole-exome sequencing, a biallelic p.Cys120Arg mutation in ectonucleotide pyrophosphatase/phosphodiesterase 1 (ENPP1) was identified in all patients. We found that this mutation, like those causing dominant Cole disease, impairs homodimerization of the ENPP1 enzyme that is mediated by its two somatomedin-B-like domains. Histological analysis revealed structural and molecular changes in affected skin that were likely to originate from defective melanocytes because keratinocytes do not express *ENPP1*. Consistently, RNA-sequencing analysis of patient-derived primary melanocytes revealed alterations in melanocyte development and in pigmentation signaling pathways. We therefore conclude that germline *ENPP1* cysteine-specific mutations, primarily affecting the melanocyte lineage, cause a clinical spectrum of dyschromatosis, in which the p.Cys120Arg allele represents a recessive and more severe form of Cole disease.

Journal of Investigative Dermatology (2018) **138,** 291–300; doi:10.1016/j.jid.2017.08.045

INTRODUCTION

Dyschromatoses are a group of skin disorders characterized by the coexistence of hyper- and hypopigmented macules (Vachiramon et al., 2011). Multiple forms of dyschromatosis have been classified based on pigmentation pattern and genetic etiology, including dyschromatosis universalis hereditaria (DUH1: OMIM 127500; DUH2: OMIM 612715; DUH3: OMIM 615402), dyschromatosis symmetrica hereditaria (OMIM 127400), and Dowling-Degos disease (OMIM 179850) (Online Mendelian Inheritance in Man, 2000). So far, only *ABCB6* on chromosome 2q36, which encodes the ATP-binding cassette subfamily B member 6 protein, has been identified as the causative gene of DUH3 (Liu et al., 2014; Zhang et al., 2013).

In this study, we identified an autosomal recessive disease characterized by the presence of hypo- and hyperpigmented lesions associated with punctate palmoplantar keratosis in eight patients. Despite similarities with some forms of DUH, the presence of mild keratoderma suggests that it should be classified as a separate entity (Table 1). The causative mutation was mapped to a cysteine-specific missense variant p.Cys120Arg in the *ENPP1* gene located on chromosome 6q23.

ENPP1 encodes ectonucleotide pyrophosphatase/phosphodiesterase 1, a transmembrane enzyme that exists as a homodimer of 230–260 kDa. It catalyzes the hydrolysis of ATP to AMP to produce extracellular inorganic pyrophosphate (Stefan et al., 2005). By generating inorganic pyrophosphate, ENPP1 acts as a key regulator of tissue calcification and bone development. In humans, homozygous loss-of-function mutations in *ENPP1* have been shown to cause several inherited disorders featuring either ectopic calcifications or abnormal calcium handling, including generalized arterial calcification of infancy (OMIM 208000), pseudoxanthomaelasticum (OMIM 264800), and autosomal recessive hypophosphatemic rickets type 2 (OMIM 613312) (Lorenz-Depiereux et al., 2010; Online Mendelian Inheritance in Man, 2000). Germline heterozygous cysteine-specific mutations in *ENPP1* were also reported to cause Cole disease (OMIM 615522) (Eytan et al., 2013; Schlipf et al., 2016; Online Mendelian Inheritance in Man, 2000), a genodermatosis featuring punctate palmoplantar

[1]*Laboratory of Human Genetics and Embryology, Institute of Medical Biology, A*STAR, Singapore, Singapore;* [2]*Laboratory of Human Cytogenetic, Molecular Genetics and Reproductive Biology, Farhat Hached University Hospital, Sousse, Tunisia;* [3]*L'Oréal Research & Innovation, Singapore, Singapore;* [4]*Department of Dermatology and Venerology, Farhat Hached University Hospital, Sousse, Tunisia;* [5]*Genome Institute of Singapore, A*STAR, Singapore, Singapore;* [6]*Department of Pathological Anatomy and Cytology, Farhat Hached University Hospital, Sousse, Tunisia;* [7]*Laboratory of Epithelial Biology, Institute of Medical Biology, A*STAR, Singapore, Singapore;* [8]*Laboratory of Skin Barrier, Institute of Medical Biology, A*STAR, Singapore, Singapore;* [9]*Helen Diller Comprehensive Cancer Center, University of California, San Francisco, California, USA;* [10]*L'Oréal Research & Innovation, Paris, France; and* [11]*Laboratory of Biosignaling and Therapeutics, Department of Cellular and Molecular Medicine, University of Leuven, Leuven, Belgium*

*Correspondence: Bruno Reversade, Laboratory of Human Genetics & Embryology, Institute of Medical Biology, A*STAR, 8A Biomedical Grove, Singapore 138648, Singapore. E-mail: bruno@reversade.com*

Abbreviations: ABCB6, ATP-binding cassette subfamily B member 6; DTT, dithiothreitol; DUH, dyschromatosis universalis hereditaria; ENPP1, ectonucleotide pyrophosphatase/phosphodiesterase 1; RNA-seq, RNA sequencing; SMB, somatomedin-B-like domain

Received 24 February 2017; revised 14 August 2017; accepted 16 August 2017; accepted manuscript published online 28 September 2017; corrected proof published online 8 January 2018

Table 1. Clinical differences and similarities between DUH1–DUH3 and Cole Disease

	Dyschromatosis universalis hereditaria			Cole Disease	
	DUH1	DUH2	DUH3	Recessive	Dominant
OMIM	127500	612715	615402	This manuscript	615522
Inheritance	Autosomal dominant	Autosomal recessive	Autosomal dominant	Autosomal recessive	Autosomal dominant
Age at onset	Early childhood (<6 y)	Early childhood (<6 y)	Early childhood (<6 y)	The first 3 mo of life	Early onset (<1 y)
Lesions	Hyper- and hypopigmented macules	Hyper- and hypopigmented macules	Hyper- and hypopigmented macules	Hyper- and hypopigmented macules, Atopic eczema	Hypopigmented macules
Location of lesions	All the body (± face)	All the body (± face)	All the body (± face)	All the body excluding the face	The extremities
Size of macules	Small hypopigmented macules interspersed with small hyperpigmented macules (<11 mm)	Small hypopigmented macules interspersed with small hyperpigmented macules (<11 mm)	Small hypopigmented macules interspersed with small hyperpigmented macules (<11 mm)	Wide hypopigmented macules (60 mm) interspersed with small hyperpigmented macules	Guttate hypopigmented macules
Punctate palmoplantar keratosis	–	–	–	+	+
Locus or *gene*	6q24.2-q25.2	12q21-23	*ABCB6* (2q36)	*ENPP1* (6q23.2) SMB1 domain	*ENPP1* (6q23.2) SMB1 and SMB2 domains
Reference	(Suzuki et al., 2005)	(Stuhrmann et al., 2008)	(Zhang et al., 2013)	This manuscript	(Eytan et al., 2013; Schlipf et al., 2016)

ABCB6, ATP-binding cassette subfamily B member 6; *ENPP1*, ectonucleotide pyrophosphatase/phosphodiesterase 1; SMB, somatomedin-B-like domain.

keratosis, patchy hypopigmentation on the extremities, and seldom cutaneous calcifications. Thus far, Cole disease has been reported to strictly follow a dominant mode of inheritance (Cole, 1976; Vignale et al., 2002).

However, because of the similarities in symptoms and cysteine-specific mutations in the same causative gene *ENPP1*, we believe that the eight patients presented herein suffer from a recessive and more extensive form of Cole disease.

RESULTS AND DISCUSSION

Clinical presentation

Eight patients with pigmentation abnormalities originating from the same Tunisian city of Sousse were investigated. Two of them have been previously reported (Kenani et al., 2008). The disease inheritance in the three unrelated families was autosomal recessive with healthy parents having multiple affected siblings of both genders (Figure 1a).

All patients displayed similar clinical features. Generalized hyper- and hypopigmented macules were present on the body sparing the face, and appeared within the first 3 months of life in all patients (Figure 1b–d). There were no apparent erythema, telangiectasia, or cutaneous calcification abnormalities. Patients' hair, nails, teeth, and mucosa appeared normal. All eight subjects developed up to 60-mm-wide hypopigmented macules on the extremities (Figure 1b–e), whereas on the trunk hypopigmented macules were guttate and interspersed with hyperpigmented macules smaller than 5 mm (Figure 1f). Patients did not have any systemic disorder or metabolic abnormalities such as diabetes. Similar to previous descriptions of Cole disease, painless punctate palmoplantar keratosis was documented in all affected children (Figure 1g) (Cole, 1976; Eytan et al., 2013). With varying onset, all patients went on to develop atopic eczema (Figure 1d and e). In contrast to the dominant form of Cole disease, heterozygous parents and carrier siblings were unaffected and did not present with any pigmentation abnormalities (Schlipf et al., 2016).

Identical-by-descent Single-nucleotide polymorphism mapping and whole-exome sequencing

Genomic DNA was isolated from the peripheral blood of all members of family 2 and genotyped on the Illumina OmniZhonghua-8 v1.0 BeadChip array. Identical-by-descent homozygosity mapping revealed a single candidate locus of 4.37 Mb on chromosome 6q (GRCh37/hg19) (Figure 2a). This region does not overlap with the 6q24.2-25.2 locus (Table 1) previously identified to segregate with DUH1 (Suzuki et al., 2005). Whole-exome sequencing analysis was also performed for four patients (II:1, II:5, II:6, II:10) (Figure 1a). One microgram of genomic DNA from each patient was processed using the NimblegenSeqCap EZ Exome v3 kit (Roche, Pleasanton, CA). Variants were called using the Genome Analysis Toolkit v2 Unified Genotyper and filtered for rare (minor allele frequency < 1%) homozygous mutations located within the chromosome 6q segment. A unique missense variant in the *ENPP1* gene (c.358T>C; p.Cys120Arg) was identified in all four patients (Figure 2a). This variant has never been reported in the 1000 Genomes project, in the exome variant server, and in the Exome Aggregation Consortium.

This private germline *ENPP1* mutation was validated by Sanger sequencing. All affected individuals were found to be homozygous, whereas unaffected parents and siblings were heterozygous or noncarriers, suggesting that it is a founder mutation unique to this Tunisian population. The c.358T>C mutation in *ENPP1* leads to a cysteine to arginine substitution

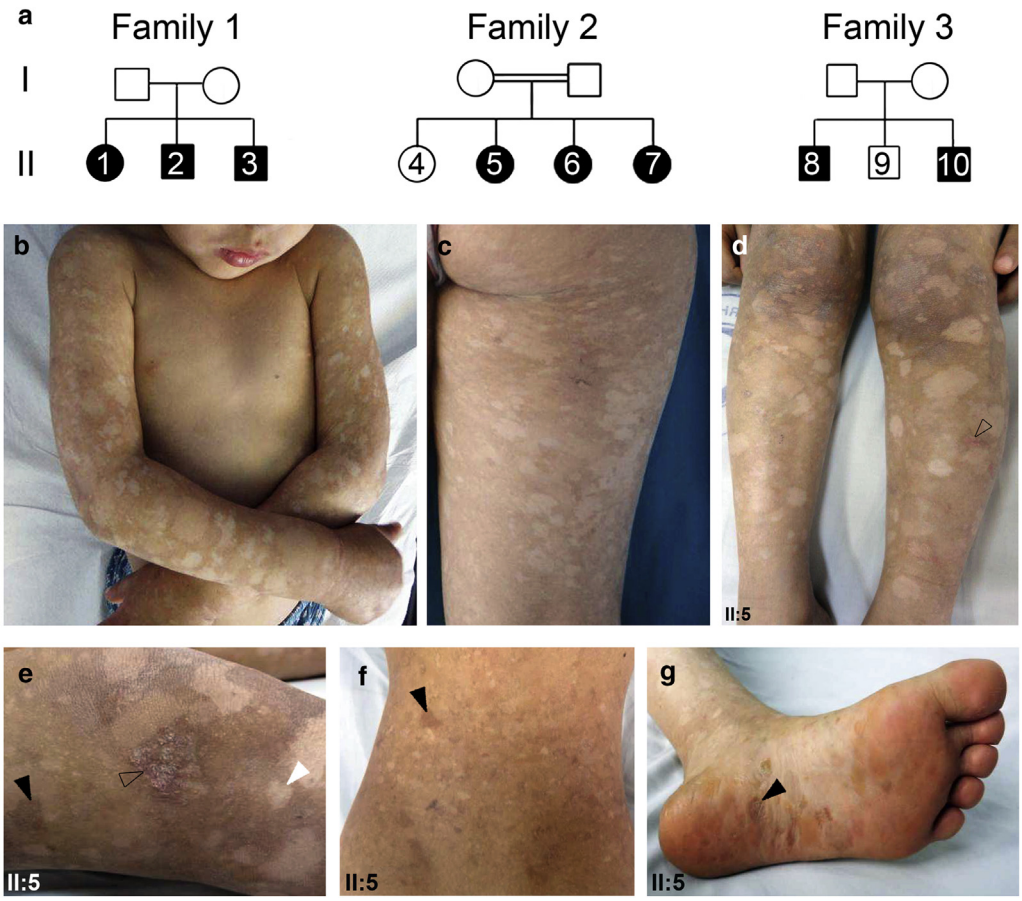

Figure 1. Clinical manifestations of autosomal recessive Cole disease in eight patients. (**a**) Pedigrees of three Tunisian families segregating autosomal recessive Cole disease (■: affected male, □: healthy male, ●: affected female, ○: healthy female). (**b**) (II:8), (**c**) (II:1), (**d**) (II:5), and (**e**) (II:5): wide hypopigmented macules on the upper and lower extremities (white arrowheads) with atopic eczema (open arrowheads). (**f**) (II:5): on the trunk the hypopigmented macules were guttate interspersed with hyperpigmented macules (black arrowheads). (**g**) (II:5): discrete yellow keratotic papules on soles (black arrowheads). All patients and guardians gave their consent to the publication of these photographs.

at position 120. This disrupts a highly conserved intrachain cystine bond within the somatomedin-B-like domain 1 (SMB1) of the ENPP1 enzyme (Gijsbers et al., 2001). ENPP1 enzyme has two SMB domains. Four cysteine-specific mutations in the SMB domains of ENPP1 have been reported as causative for dominant Cole disease, three of which lie in the SMB2 domain (Figure 2b, indicated in blue) (Eytan et al., 2013; Schlipf et al., 2016). These three heterozygous variants affecting conserved cysteine residues (p.Cys149, p.Cys164, and p.Cys177) segregate with dominant Cole disease (Schlipf et al., 2016). In contrast, the mutation causing the p.Cys120Arg change in the SMB1 domain must be biallelic to cause the recessive disease (Figure 2b, indicated in red). It is noteworthy that p.Cys120 residue within SMB1 is analogous in its position and disulfide bridging to p.Cys164 in SMB2 (Figure 2c), yet mutations in these two domains lead to distinct inheritance patterns. This suggests that the two domains are not equivalent and may play distinct roles in ENPP1 function.

Our patients present with many of the clinical symptoms typically associated with patients suffering from dominant Cole disease (Table 1), and both carry germline *ENPP1* cysteine-specific mutations. Therefore, we propose that these two genodermatoses represent a clinical spectrum of Cole disease and classify to our knowledge this previously unreported variant as a recessive form of Cole disease (Table 1).

Histological and structural changes in recessive Cole disease skin

To establish full histological and structural interpretation of patient skin, we obtained skin biopsies encompassing both hyper- and hypopigmented lesions from patient II:5 and her healthy noncarrier sibling II:4. The skin biopsies were obtained from the same location at the lower back.

Despite presenting a normal stratum corneum, the hematoxylin and eosin staining showed a thicker epidermis with more pronounced dermal papillae in patient skin, as compared with control skin (Figure 3a and b). In line with their clinical appearance, both hematoxylin and eosin and Fontana-Masson staining of patient skin revealed an increased pigmentation in the epidermal basal layer with a slightly increased number of melanocytes in the hyperpigmented region and a reduced pigmentation in the grossly hypopigmented area relative to control skin (Figure 3a–d). The presence of perivascular inflammatory cells in the papillary dermis of affected skin was not significant but an increased number of pigmented dermal dendrocytes could be seen (Figure 3a–d).

To better understand the origin of the observed pigmentation abnormalities, Melan A was used as a marker for melanocyte numbers (Figure 3e and f), and tyrosinase (Figure 3g and h), microphthalmia-associated transcription factor (Figure 3i and j), and tyrosinase-related protein 1 (Figure 3k and l) were used to assess melanogenesis activity. All markers showed upregulation in hyperpigmented regions and

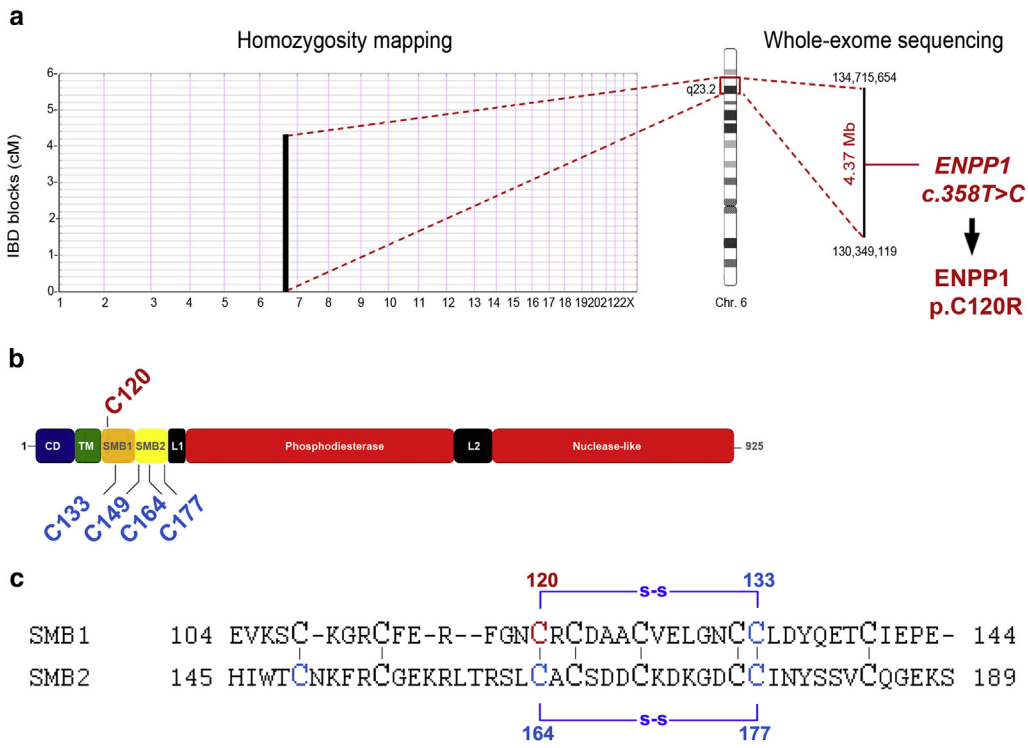

Figure 2. A homozygous p.Cys120Arg mutation in ENPP1 is responsible for recessive Cole disease. (**a**) Identical-by-descent single-nucleotide polymorphism mapping followed by whole-exome sequencing delineates one locus on chromosome 6q shared by all studied propositi. The homozygous *ENPP1* missense mutation c.358T>C (p.Cys120Arg) segregates with the disease. (**b**) Comparison of dominant and recessive Cole disease mutated cysteines in SMB domains. The biallelic mutated cysteine responsible for the recessive form (indicated in red) is located in the SMB1 domain, whereas three of four heterozygous mutations causing the dominant form affect cysteine residues located within SMB2 (indicated in blue). (**c**) The pairing and spacing of the eight cysteines of SMB domains of ENPP1 are conserved. Cysteine bonds between p.Cys120/Cys133 in SMB1 and p.Cys164/Cys177 in SMB2 are analogous yet cause different inheritance patterns when mutated. ENPP1, ectonucleotide pyrophosphatase/phosphodiesterase 1; SMB, somatomedin-B-like domain.

downregulation in hypopigmented regions, as compared with normal skin, supporting an impaired melanogenesis activity in the patient's skin. We also stained for human melanoma black 45, a marker for immature melanosomes, and found that the staining intensity was comparable in all skin samples (Figure 3m and n).

To further examine general structural changes in the patient's skin, specific markers were assessed by immunohistochemistry regardless of pigmentation status. Elastin fibers were found noticeably increased in the patient's dermis, as compared with healthy skin (Supplementary Figure S1a and b online). The expression of two cytokeratin markers, cytokeratin 14 and cytokeratin 10, was lower in the basal and suprabasal epidermis of the affected skin as compared with control (Supplementary Figure S1c–f). The staining intensity of the proliferation marker Ki67 was noticeably higher in the patient's skin (Supplementary Figure S1g and h). Taken together, these results suggest that epidermal differentiation and stratification processes could be altered in the affected skin, which could contribute to the presence of punctate palmoplantar keratosis in our patients. Additional staining with Laminin and E-cadherin showed that the dermal-epidermal junction was normal in all skin specimens (Supplementary Figure S1i–l).

Because ENPP1 was shown to play an important role in the stimulator of interferon genes innate immune pathway by hydrolyzing the second messenger 2′3′-cGAMP (Li et al., 2014), specific immune system markers were examined by immunohistochemistry. There was no significant inflammatory infiltrate in the patient's skin, although an increased number of cluster of differentiation 3-positive T cells in the papillary dermis were seen as compared with control (Supplementary Figure S2a and b online). The number of Factor XIIIA-positive cells was slightly elevated in the affected dermis (Supplementary Figure S2c and d), indicating an increase in the number of monocytes and/or macrophages. Finally, there was no obvious difference in the number of epidermal cluster of differentiation 1a-expressing Langerhans cells across all samples studied (Supplementary Figure S2e and f).

Although we were able to examine only one skin lesion by immunohistochemistry, these results provide a good assessment of the cellular and molecular changes occurring in the skin of a patient with recessive Cole disease relative to her healthy sibling.

ENPP1 is specifically expressed in melanocytes but not in keratinocytes

To examine ENPP1 expression in the human skin, we performed immunohistochemistry staining using a validated mouse mAb against ENPP1 (Gijsbers et al., 2001). Endogenous ENPP1 was detected in the basal layer of the epidermis and in the dermis of healthy skin collected from unaffected sibling II:4 and patient II:5 (Figure 4a and b). We next evaluated *ENPP1* expression by Q-PCR in different primary skin cells generated from a skin biopsy of an ethnically matched healthy control. *ENPP1* transcript was detected in primary fibroblasts ($P = 0.0006$) and melanocytes ($P = 0.0007$), but not in keratinocytes (Figure 4c). This result was confirmed at the protein level by western blotting of the corresponding cellular extracts using the same ENPP1 mAb (Figure 4c). Keratin 14, *collagen type I alpha 1*, and *melanocortin 1 receptor* were measured to confirm the identity of each cell type (Supplementary Figure S3a and b online).

To investigate whether the missense variant c.358T>C could affect endogenous ENPP1 expression in patient cells, we assessed its levels in primary fibroblasts and melanocytes

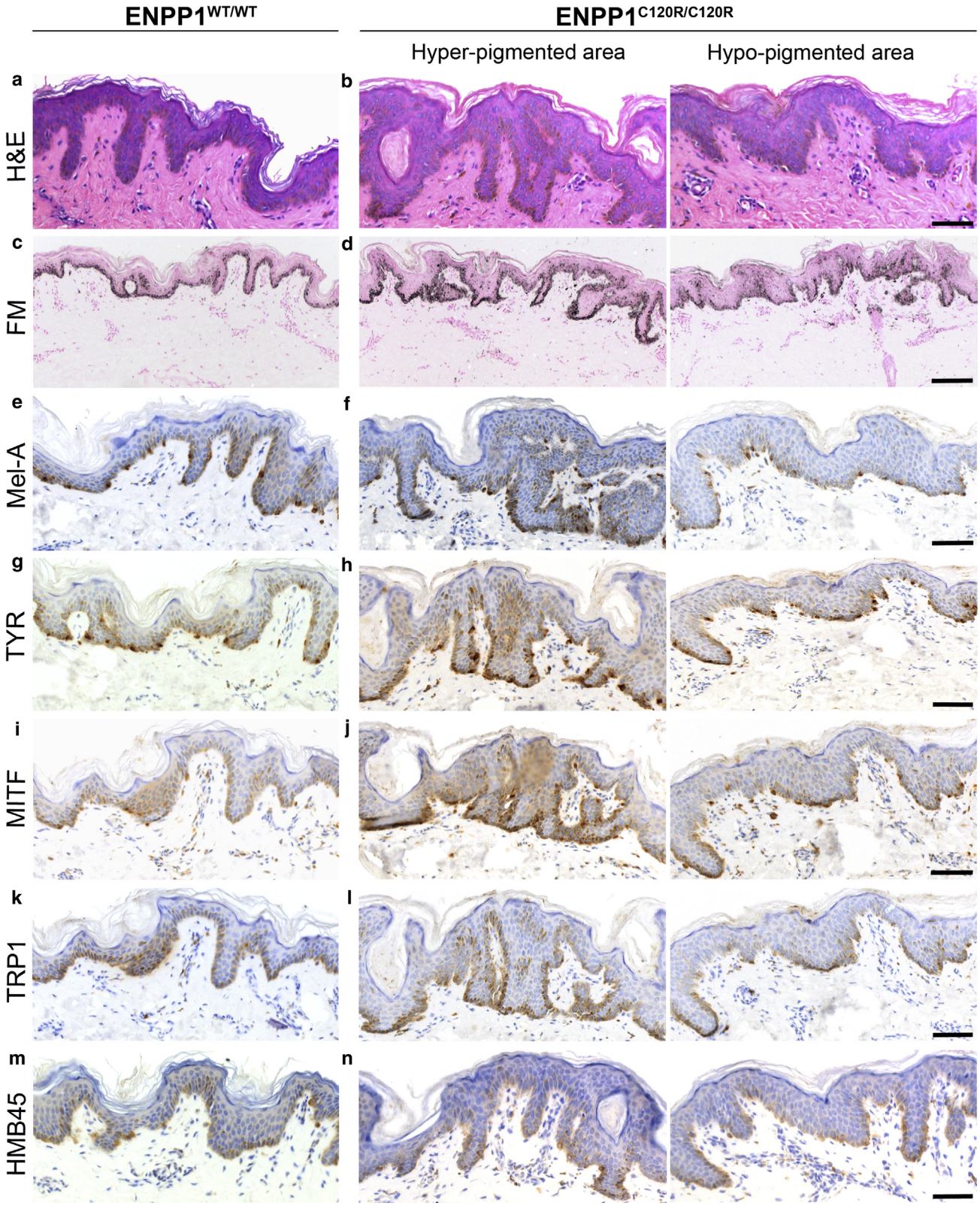

Figure 3. Histological and molecular changes in the hyper- and hypopigmented patient's skin. Histopathological and immunohistochemical examination of skin biopsies from hyper- and hypopigmented lesions of patient II:5 ($ENPP1^{C120R/C120R}$) (middle and right panels) and from her healthy sibling II:4 ($ENPP1^{WT/WT}$) (left panels). (**a, b**) Representative hematoxylin and eosin stained skin sections from the control and patient. (**c, d**) FM staining of patient skin sections compared with control. (**e**–**n**) Immunohistochemistry staining of control and patient skin sections using (**e, f**) anti-Mel-A, (**g, h**) anti-TYR, (**i, j**) anti-MITF, (**k, l**) anti-TRP1, and (**m, n**) anti-HMB45. Scale bar = 50 μm except panel **c** and **d** scale bar = 125 μm. ENPP1, ectonucleotide pyrophosphatase/phosphodiesterase 1; FM, Fontana-Masson; HMB45, HMB45, human melanoma black 45; Mel-A, Melan A; MITF, microphthalmia-associated transcription factor; TRP1, tyrosinase-related protein 1; TYR, tyrosinase.

derived from patient II:8. There were no significant differences in *ENPP1* transcript levels between control and patient fibroblasts (Figure 4d). However, *ENPP1* expression was significantly downregulated in patient melanocytes, as compared with control ($P = 0.005$) (Figure 4e). We also noted that the expression of *melanocortin 1 receptor,* a key regulator of melanogenesis, was significantly reduced in patient melanocytes, as compared with control ($P = 0.002$) (Supplementary Figure S3c). The endogenous ENPP1 protein level in control and patient fibroblasts was verified using the same ENPP1 mAb (Figure 4i). Interestingly, two custom polyclonal rabbit antibodies raised against the epitope (CFERFGNRRCDAA) encompassing the mutated cysteine could recognize the endogenous wild-type, but not mutated ENPP1 protein (Figure 4i), indicating that the SMB1 domain structure is severely affected by the biallelic p.Cys120Arg mutation. Because keratinocytes are devoid of endogenous ENPP1 expression, our data suggest that melanocytes are likely to be the cell of origin and therefore the main epidermal lineage driving the pathogenesis of recessive and dominant Cole disease.

Effect of C120R and C164S mutations on ENPP1 dimerization

ENPP1 is a transmembrane enzyme with a short cytoplasmic region and a large extracellular domain consisting of two consecutive SMB domains: a phosphodiesterase domain and a nuclease-like domain that lacks catalytic activity (Goldfine et al., 2008). The phosphodiesterase domain cleaves a variety of chemical bonds including sugar phosphate, pyrophosphate, and phosphodiester (Terkeltaub et al., 1994). The SMB domains contain eight cysteine residues, each arranged in four disulphide bonds, and have been shown to mediate ENPP1 homodimerization through covalent cystine inter- and intramolecular bonds (Bellacchio, 2012; Gijsbers et al., 2003). To investigate the effect of the patient Cys120Arg mutation on ENPP1 dimerization, we transiently transfected HEK293T cells with either $ENPP1^{WT}$, $ENPP1^{C120R}$, or $ENPP1^{C164S}$ constructs. The p.Cys164Ser mutation in the SMB2 domain is responsible for the dominant form of Cole disease and is analogous to the p.Cys120 of the SMB1 domain with respect to its disulphide bonding. Overexpressed ENPP1 was revealed with antibodies raised against the N-terminus or C-terminus of ENPP1 under reducing and nonreducing conditions. Untransfected HEK293T cells did not express endogenous ENPP1 (Figure 4f and g, lane 1). In the presence of dithiothreitol (DTT) that breaks intra- and intermolecular disulphide bonds, we detected ENPP1 as a monomer at the expected size of approximately 130 kDa for both $ENPP1^{WT}$ and $ENPP1^{C120R}$. We also observed an additional lower band for the two mutated ENPP1 monomers, reflecting possible aberrant post-translational modifications (Figure 4f and g, DTT, lanes 2–4). Under nonreducing conditions, no bands corresponding to the monomer were detectable for all three extracts, which is consistent with disulphide-mediated oligomerization of ENPP1. A visible homodimer was observed at the expected size of approximately 260 kDa for $ENPP1^{WT}$ (Figure 4f and g, no DTT, lane 2). Although $ENPP1^{C120R}$ was less prone to dimer formation relative to $ENPP1^{WT}$ (Figure 4f and g, no DTT, lane 4), $ENPP1^{C164S}$ dimer formation was the weakest (Figure 4f and g, no DTT, lane 3), suggesting that the Cys164Ser mutation severely affects ENPP1 dimerization. Additional high molecular weight bands could be clearly documented in both mutated ENPP1 but not for wild-type ENPP1 and were consistent using anti-N- or C-termini ENPP1 antibodies (Figure 4f and g). These high molecular bands could be due to the formation of misfolded ENPP1 homomultimer or aberrant covalent interactions with other proteins. The validated mAb could only recognize $ENPP1^{WT}$ under nonreducing conditions (Figure 4h). In this heterologous HEK293T assay, the p.Cys164Ser mutation responsible for dominant Cole disease severely affected dimer formation, whereas the p.Cys120Arg responsible for recessive Cole disease retained partial ENPP1 dimerization. This raises the possibility that differential requirements for these analogous cysteines may explain the dominant versus recessive inheritance pattern of this disease.

RNA-sequencing analysis of patient-derived melanocytes

Because melanogenesis is impaired in the patient's skin, we used next-generation RNA sequencing (RNA-seq) to characterize the transcriptional changes in patient-derived primary melanocytes. RNA-seq was performed using mRNA extracted from primary hypo- and hyperpigmented melanocytes isolated from patient II:8, melanocytes from his healthy heterozygous sibling II:9, and an aged and ethnically matched control.

To confirm the identity of our melanocyte cultures, we compared our datasets with 13 publicly available transcriptomes from various human cell types (Supplementary Table S1 online). Indeed, the four primary melanocyte lines used in our study clustered tightly with other human melanocyte lines and were clearly distinct from other skin cell types including fibroblasts or keratinocytes (Figure 5a). We examined the data from our primary melanocyte lines using principal component analysis. Through unsupervised clustering of normalized transcript levels, the mutant hypopigmented melanocytes could be readily distinguished from the hyperpigmented mutant cells as well as from the two controls that clustered together (Figure 5b).

A pairwise fold-change comparison was then performed, and genes were computationally filtered using a cutoff of more than 2 fold-change and $P < 0.01$. We first compared hyperpigmented melanocytes with each control individually and then overlapped the results to obtain a high confidence list of differentially expressed genes (Figure 5c). The same analysis was repeated for hypopigmented cells (Figure 5e). Finally, to obtain a profile of the overall differential gene expression, downregulated genes in hyper- and hypopigmented cells were overlapped to identify 143 genes that were downregulated in patient melanocytes compared with controls regardless of pigmentation status (Figure 5g). Similar analysis was performed to obtain a list of 172 upregulated genes (Figure 5g). These results are publicly accessible under Gene Expression Omnibus number GSE93657 and are tabulated in Supplementary Table S2 online.

To examine the functional consequences of gene expression changes associated with C120R mutation, the differentially expressed gene lists were explored using Ingenuity Pathways Analysis Software (Ingenuity Systems, http://www.

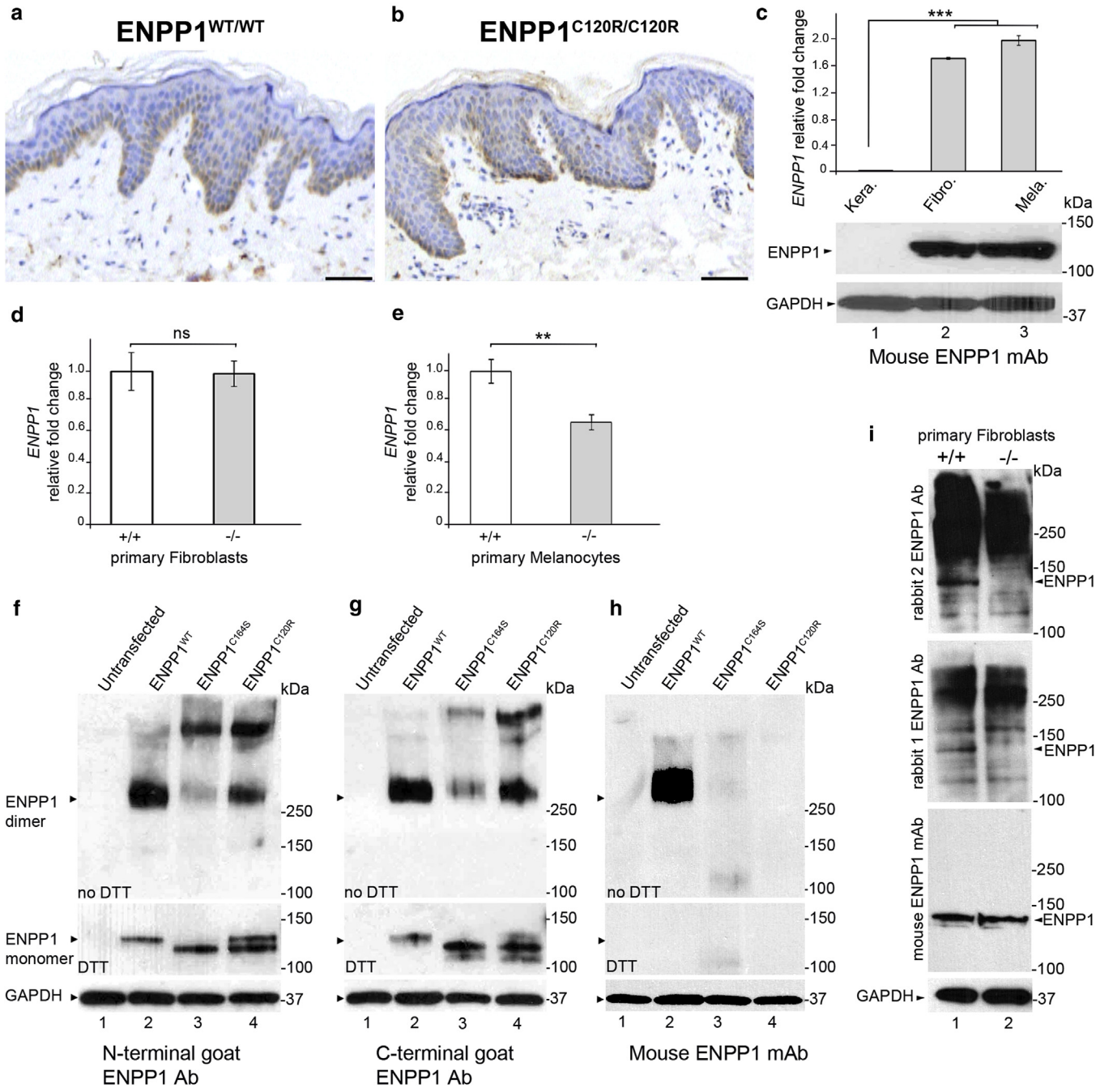

Figure 4. ENPP1 is expressed in melanocytes and the p.Cys120Arg mutation impairs its dimerization. (**a, b**) Immunohistochemistry staining in skins obtained from healthy individual II:4 and patient II:5 using a mouse mAb against ENPP1; scale bar = 50 μm. (**c**) *ENPP1* mRNA level in primary keratinocytes, fibroblasts, and melanocytes. Endogenous ENPP1 protein expression was analyzed in primary skin cells using the same ENPP1 mAb. (**d, e**) *ENPP1* expression in control and patient II:8 fibroblasts and melanocytes. Data plotted as mean ± SEM of three independent replicates, $^{**}P \leq 0.01$; $^{***}P \leq 0.001$. (**f, g, h**) Representative blots of overexpressed ENPP1^{WT}, ENPP1^{C164S}, or ENPP1^{C120R}. Membranes were probed either in the presence or absence of DTT, with N- or C-termini ENPP1 polyclonal antibodies, or mouse ENPP1 mAb. (**i**) Endogenous ENPP1 protein expression was analyzed in control and patient fibroblasts using ENPP1 mAb and two custom rabbit polyclonal antibodies. GAPDH was used as a loading control. DTT, dithiothreitol; ENPP1, ectonucleotide pyrophosphatase/phosphodiesterase 1; Fib, fibroblasts; GAPDH, glyceraldehyde-3-phosphate dehydrogenase; Kera, keratinocytes; Mela, melanocytes.

ingenuity.com). Ingenuity Pathways Analysis highlighted several pathways that appeared to be altered in hypo- and hyperpigmented cells. Among these, melanocyte development and pigmentation signaling pathways (Supplementary Table S3 online) were found to be altered for both mutant cells. We selected 36 deregulated genes for detection by Q-PCR (Figure 5d, f, and h) and were able to validate 32, indicating the reliability of our RNA-seq data. Most of the selected genes are associated with skin pigmentation pathways (Supplementary Table S3).

Ingenuity Pathways Analysis also revealed a significant upregulation of several pathways related to oxidative phosphorylation in hyperpigmented melanocytes (Supplementary Table S4 online), which could be an effect of the high rate of

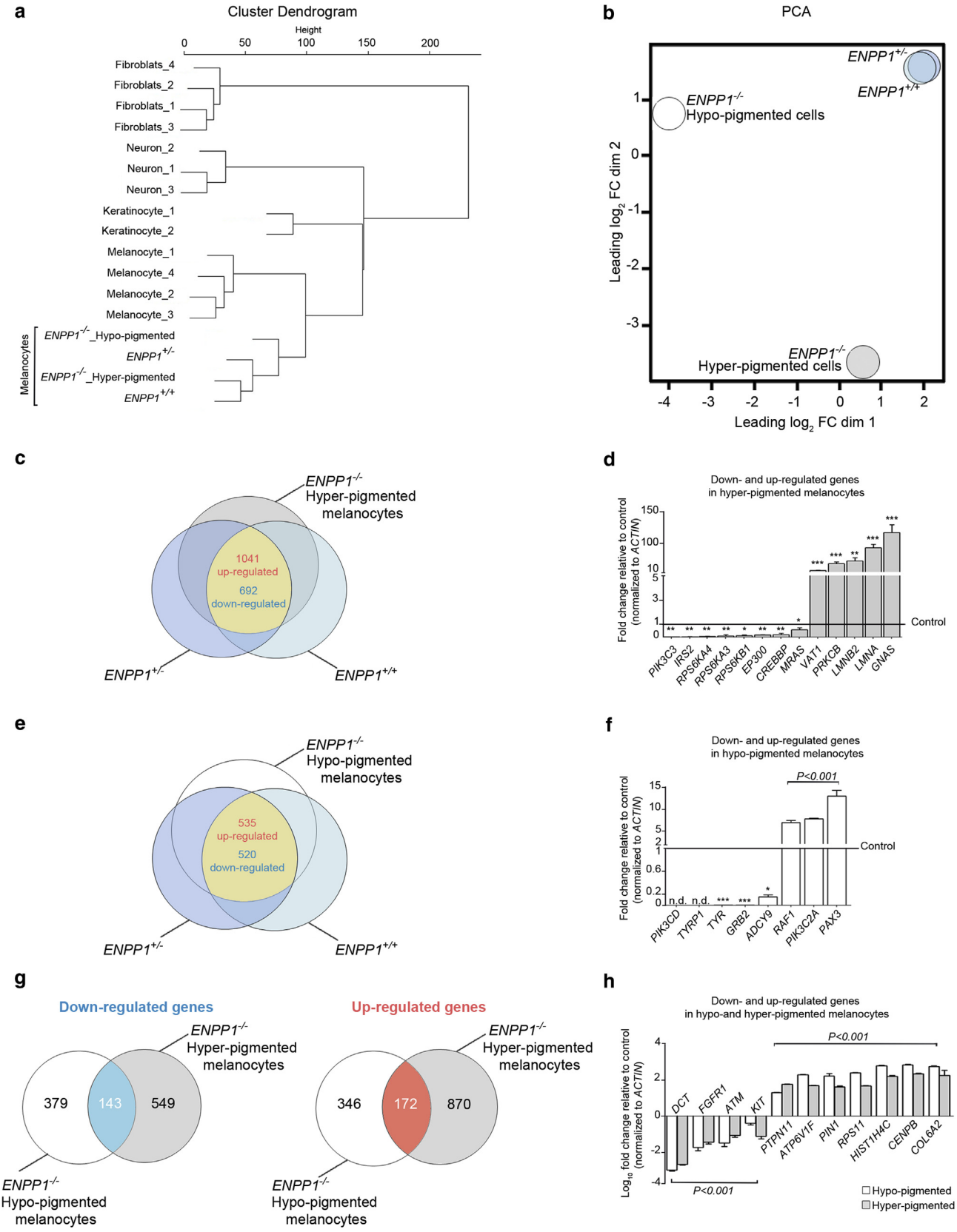

Figure 5. RNA-seq analysis of patient-derived melanocytes reveals altered melanogenesis. RNA-seq data of mutant melanocytes (hypo- and hyperpigmented) versus two controls (*ENPP1*$^{+/-}$ and *ENPP1*$^{+/+}$) melanocytes. (**a**) Hierarchical cluster dendrogram of isolated melanocytes used in our study compared with 13 publicly available human cell lines. (**b**) PCA of unsupervised clustering of mutant melanocytes compared with controls. (**c, e**) Venn diagrams illustrating the number of differentially expressed genes in hyper- and hypopigmented melanocytes (>2-fold, $P < 0.01$). (**d**) Venn diagrams of differentially expressed genes in mutant melanocytes regardless of pigmentation status. (**d, f, h**) Validation of selected genes from RNA-seq by Q-PCR. Data are shown as mean ± standard

melanin synthesis in these cells. It is known that the by-products of melanin synthesis cause oxidative stress in human epidermal melanocytes and, when accumulated, can lead to cell death (Fried and Arbiser, 2008). Several hormone and growth factor signaling pathways were downregulated in hyperpigmented cells (Supplementary Table S4). On the other hand, signal transduction pathways involved in translation regulation were upregulated in hypopigmented melanocytes (Supplementary Table S4), which could indicate a higher proliferation rate in these melanocytes. Vesicular trafficking pathways were downregulated in hypopigmented melanocytes as compared with control cells, which could affect melanosome transport in these cells. On further analysis, several genes involved in skin pigmentation such as *dopachrometautomerase, fibroblast growth factor receptor 1, ATM serine/threonine kinase,* and *proto-oncogene receptor tyrosine kinase* were overall downregulated in mutant melanocytes regardless of the pigmentation status (Figure 5h). It is unclear whether this is directly due to the homozygous Cys120Arg mutation, but it may explain the pervasive presence of hypopigmented skin lesions in our patients. To conclude, our RNA-seq provides further evidence that *ENPP1* plays a critical role in the skin pigmentation process in humans.

To date, most of the reported germline *ENPP1* mutations are associated with generalized arterial calcification of infancy or autosomal recessive hypophosphatemic rickets type 2. These mutations affect either the active phosphodiesterase domain or the inactive nuclease domain of ENPP1 (Lorenz-Depiereux et al., 2010). However, the germline Cys120Arg substitution identified herein lies within the SMB1 domain. Other cysteine mutations in the SMB2 domain are associated with the dominant form of Cole disease, suggesting that the two SMB domains of ENPP1 play a critical role in epidermal differentiation and skin pigmentation. It has been suggested that ENPP1 can inhibit insulin receptor autophosphorylation and downstream signaling through its SMB1 and SMB2 domains (Dimatteo et al., 2013). This interplay between ENPP1 and the inhibit insulin receptor may be a future line of investigation to understand the pathogenesis of Cole disease.

In summary, we present a hitherto unknown variant of Cole disease with a recessive inheritance pattern that is characterized by the presence of hypo- and hyperpigmented lesions over the whole body (Table 1). Both recessive and dominant Cole diseases are caused by germline cysteine-specific mutations that impact ENPP1 homodimerization specifically in melanocytes. These two monogenic genodermatoses represent a clinical spectrum of dyschromatosis, where the recessive form reported herein represents a more severe and extensive form of Cole disease.

MATERIAL AND METHODS

Subjects and informed consent

All participants in this study provided written informed consent. The clinical diagnosis of DUH was confirmed in all patients by two experienced dermatologists. Skin biopsies were obtained from individuals: II:4, II:5, II:8, II:9, and from an ethnically matched control. Peripheral blood samples were collected from eight affected and eight unaffected members from the three families for genomic DNA extraction. The study protocol was approved by the Tunisian and Singaporean Institutional Review Board (NUS IRB 10-051). All patients gave their consent to publish their photographs.

Identification of causative gene

Identical-by-descent homozygosity mapping, whole exome sequencing, and Sanger sequencing are detailed in Supplementary Materials and Methods online.

Patient biopsies histopathology and immunohistochemistry

Two skin biopsies were obtained from the lower back (not sun exposed regions) of affected (II:5) and unaffected (II:4) sibling for histopathology purposes. Primary skin cells were isolated from fresh skin biopsies obtained from patient II:8, his healthy sibling II:9, and an ethnically matched healthy control. Biopsy procedures and immunohistochemistry staining are detailed in Supplementary Materials and Methods.

Quantitative PCR

Total RNA was extracted from primary skin cells using the RNeasy Mini Kit (QIAGEN). One microgram of RNA was reverse transcribed using the 5X iScript RT Super Mix (Bio RAD). Q-PCR was performed using a 7900HT Fast Real Time PCR System (Applied Biosystems) following the manufacturer's protocols. Housekeeping gene *BETA-ACTIN* was used for normalization. For RNA-seq validation (Figure 5), the expression level of each gene was compared with control and normalized to *BETA-ACTIN*. Primer sequences are listed in Supplementary Table S5 online.

Cloning of expression vectors, cell transfections, and western blotting

Cloning details, protocols for transient HEK293T transfection, protein extraction, and western blotting analysis are detailed in Supplementary Materials and Methods.

RNA sequencing

The samples were first depleted of ribosomal RNA using the Low Input RiboMinus Eukaryote v2 kit from Thermo Fischer Scientific, and then processed using the NEBNext Ultra RNA Directional

deviation, $*P \leq 0.05$; $**P \leq 0.01$; $***P \leq 0.001$. *PIK3CD* and *TYRP1* mRNA were detected in control but not in mutant melanocytes (fold-change and *P* value could not be calculated; n.d: not detected). ADCY9, adenylatecyclase 9; ATM, ATM serine/threonine kinase; ATP6V1F, ATPase H+ transporting V1 subunit F; CENPB, centromere protein B; COL6A2, collagen type VI alpha 2; CREBBP, cAMP-response element binding protein; DCT, dopachrometautomerase; ENPP1, ectonucleotide pyrophosphatase/phosphodiesterase 1; EP300, E1A binding protein p300; FGFR1, fibroblast growth factor receptor 1; GNAS, guanine nucleotide-binding proteins; GRB2, growth factor receptor bound protein 2; HIST1H4C, histone cluster 1, H4c; IRS2, insulin receptor substrate 2; KIT, proto-oncogene receptor tyrosine kinase; LMNA, lamin A; LMNB2, lamin B2; MRAS, muscle RAS oncogenehomolog; PAX3, paired box 3; PCA, principal component analysis; PIK3C2A, phosphatidylinositol-4-phosphate 3-kinase catalytic subunit type 2 alpha; PIK3C3, phosphatidylinositol 3-kinase catalytic subunit type 3; PIK3CD, phosphatidylinositol-4,5-bisphosphate 3-kinase catalytic subunit delta; PIN1, peptidylprolylcis/trans isomerase NIMA-interacting 1; PRKCB, protein kinase C beta; PTPN11, protein tyrosine phosphatase non-receptor type 11; RAF1, Raf-1 proto-oncogene serine/threonine kinase; RPS11, ribosomal protein S11; RPS6KA3, ribosomal protein S6 kinase A3; RPS6KA4, ribosomal protein S6 kinase A4; RPS6KB1, ribosomal protein S6 kinase B1; TRP1, tyrosinase-related protein 1; VAT1, vesicle amine transport 1.

Library Preparation kit from NEB. Full details are given in Supplementary Materials and Methods.

Statistical analysis

Each experiment was repeated at least three times, and data were expressed as mean ± standard error of the mean based on three independent replicates, except RNA-seq validation Q-PCR (Figure 5), where error bars were calculated from three technical replicates (mean ± standard deviation). The *P* values from all pairwise comparisons were calculated using two-tailed Student's *t* test. Statistical tests were performed in GraphPad Prism 6 or Microsoft Excel using the *t* test function. Statistical significance throughout the article was denoted as follows: $*P < 0.05$; $**P < 0.01$; $***P < 0.001$.

CONFLICT OF INTEREST

The authors state no conflict of interest.

ACKNOWLEDGMENTS

We are grateful to all the patients and their relatives for their contribution and participation in our study. We thank all the technicians at the department of dermatology and venereology and the technicians at the department of cytogenetic and molecular biology, CHU Farhat Hached, Sousse, Tunisia, for their help on sample collection. We would like to acknowledge Lena Ho and Franklin Zhong for their constructive feedback. We also thank AIT biotech for their technical support. MC is a PhD student in the University of Monastir in Tunisia and is funded by an A*STAR Research Attachment Program. BR is a fellow of the Branco Weiss Foundation, an A*STAR Investigator and EMBO Young Investigator. This work was partly funded by the Skin Research Institute of Singapore (SRIS) and a Strategic Positioning Fund on Genetic Orphan Diseases from A*STAR, Singapore. This work was partly funded by L'Oréal Research & Innovation Department. MSL, SL, LD, and YBK are employees of L'Oréal.

SUPPLEMENTARY MATERIAL

Supplementary material is linked to the online version of the paper at www.jidonline.org, and at https://doi.org/10.1016/j.jid.2017.08.045.

REFERENCES

Bellacchio E. In silico analysis of the two tandem somatomedin B domains of ENPP1 reveals hints on the homodimerization of the protein. J Cell Physiol 2012;227:3566–74.

Cole LA. Hypopigmentation with punctate keratosis of the palms and soles. Arch Dermatol 1976;112:998–1000.

Dimatteo C, Marucci A, Palazzo A, Cisternino C, Marsano RM, Trischitta V, et al. Role of somatomedin-B-like domains on ENPP1 inhibition of insulin signaling. Biochim Biophys Acta 2013;1833:552–8.

Eytan O, Morice-Picard F, Sarig O, Ezzedine K, Isakov O, Li Q, et al. Cole disease results from mutations in ENPP1. Am J Hum Genet 2013;93:752–7.

Fried L, Arbiser JL. The reactive oxygen-driven tumor: relevance to melanoma. Pigment Cell Melanoma Res 2008;21:117–22.

Gijsbers R, Ceulemans H, Bollen M. Functional characterization of the non-catalytic ectodomains of the nucleotide pyrophosphatase/phosphodiesterase NPP1. Biochem J 2003;371(Pt 2):321–30.

Gijsbers R, Ceulemans H, Stalmans W, Bollen M. Structural and catalytic similarities between nucleotide pyrophosphatases/phosphodiesterases and alkaline phosphatases. J Biol Chem 2001;276:1361–8.

Goldfine ID, Maddux BA, Youngren JF, Reaven G, Accili D, Trischitta V, et al. The role of membrane glycoprotein plasma cell antigen 1/ectonucleotide pyrophosphatase phosphodiesterase 1 in the pathogenesis of insulin resistance and related abnormalities. Endocr Rev 2008;29:62–75.

Kenani N, Ghariani N, Denguezli M, Sriha B, Belajouza C, Nouira R. Dyschromatosis universalis hereditaria: two cases. Dermatol Online J 2008;14:16.

Li L, Yin Q, Kuss P, Maliga Z, Millan JL, Wu H, et al. Hydrolysis of 2′3′-cGAMP by ENPP1 and design of nonhydrolyzable analogs. Nat Chem Biol 2014;10:1043–8.

Liu H, Li Y, Hung KK, Wang N, Wang C, Chen X, et al. Genome-wide linkage, exome sequencing and functional analyses identify ABCB6 as the pathogenic gene of dyschromatosis universalis hereditaria. PLoS One 2014;9:e87250.

Lorenz-Depiereux B, Schnabel D, Tiosano D, Hausler G, Strom TM. Loss-of-function ENPP1 mutations cause both generalized arterial calcification of infancy and autosomal-recessive hypophosphatemic rickets. Am J Hum Genet 2010;86:267–72.

Online Mendelian Inheritance in Man, OMIM.McKusick-Nathans Institute for Genetic Medicine, Johns Hopkins University (Baltimore, MD) and National Center for Biotechnology Information, National Library of Medicine (Bethesda, MD), 2000. http://www.ncbi.nlm.nih.gov/omim/.

Schlipf NA, Traupe H, Gilaberte Y, Peitsch WK, Hausser I, Oji V, et al. Association of Cole disease with novel heterozygous mutations in the somatomedin-B domains of the ENPP1 gene: necessary, but not always sufficient. Br J Dermatol 2016;174:1152–6.

Stefan C, Jansen S, Bollen M. NPP-type ectophosphodiesterases: unity in diversity. Trends Biochem Sci 2005;30:542–50.

Stuhrmann M, Hennies HC, Bukhari IA, Brakensiek K, Nurnberg G, Becker C, et al. Dyschromatosis universalis hereditaria: evidence for autosomal recessive inheritance and identification of a new locus on chromosome 12q21-q23. Clin Genet 2008;73:566–72.

Suzuki N, Suzuki T, Inagaki K, Ito S, Kono M, Fukai K, et al. Mutation analysis of the ADAR1 gene in dyschromatosis symmetrica hereditaria and genetic differentiation from both dyschromatosis universalis hereditaria and acropigmentatio reticularis. J Invest Dermatol 2005;124:1186–92.

Terkeltaub R, Rosenbach M, Fong F, Goding J. Causal link between nucleotide pyrophosphohydrolase overactivity and increased intracellular inorganic pyrophosphate generation demonstrated by transfection of cultured fibroblasts and osteoblasts with plasma cell membrane glycoprotein-1. Relevance to calcium pyrophosphate dihydrate deposition disease. Arthritis Rheum 1994;37:934–41.

Vachiramon V, Thadanipon K, Chanprapaph K. Infancy- and childhood-onset dyschromatoses. Clin Exp Dermatol 2011;36:833–8. quiz 9.

Vignale R, Yusin A, Panuncio A, Abulafia J, Reyno Z, Vaglio A. Cole disease: hypopigmentation with punctate keratosis of the palms and soles. Pediatr Dermatol 2002;19:302–6.

Zhang C, Li D, Zhang J, Chen X, Huang M, Archacki S, et al. Mutations in ABCB6 cause dyschromatosis universalis hereditaria. J Invest Dermatol 2013;133:2221–8.